

1 Humphreys, Madeleine C.S.¹, Edmonds, M.², Christopher, T.³ & Hards, V.⁴

2

3 ¹ Department of Earth Sciences, Durham University, Science Labs, Durham, DH1
4 3LE, UK

5 ² Department of Earth Sciences, University of Cambridge, Downing Street,
6 Cambridge, CB2 3EQ, UK

7 ³ Montserrat Volcano Observatory, Flemmings, Montserrat, West Indies

8 ⁴ British Geological Survey, Environmental Science Centre, Keyworth, Nottingham,
9 NG12 5GG

10

11 **Reply to:**

12 Magma storage region processes of the Soufrière Hills Volcano, Montserrat. Joseph D
13 Devine and Malcolm Rutherford.

14

15 **Abstract**

16 Devine & Rutherford (2014), “Magma storage region processes of the Soufrière Hills
17 Volcano, Montserrat”, published as Chapter 19 of the Geological Society of London
18 Memoir, volume 39, criticised the data and methods of Humphreys et al. (2010),
19 Magma hybridisation and diffusive exchange recorded in heterogeneous glasses from
20 Soufrière Hills Volcano, Montserrat, Geophysical Research Letters, L00E06. We
21 thoroughly review the melt inclusion dataset presented by Humphreys et al. (2010)
22 and show the results to be robust. High volatile contents inferred ‘by difference’ from
23 electron microprobe analysis are supported by direct volatile measurements in
24 multiple independent studies. Plagioclase-hosted melt inclusions in many dome lavas
25 have low H₂O contents, which we attribute to diffusive loss through the host mineral.
26 Our corrections for post-entrapment crystallisation did not introduce significant
27 artefacts into the dataset that would affect our original conclusions. Rather, the
28 anomalous minor element compositions found in a subset of our melt inclusions and
29 matrix glasses is supported by other independent studies, and can be best explained as
30 a result of mingling and hybridisation with mafic magmas that are compositionally
31 variable through time.

32

33 **Introduction**

34 The recent study by Devine & Rutherford (2014; hereafter DR2014), “Magma storage
35 region processes of the Soufrière Hills Volcano, Montserrat”, published as Chapter 19
36 of the Geological Society of London Memoir, volume 39, focused primarily on
37 updating the record of magmatic temperatures recorded by Fe-Ti oxides in the
38 andesite erupted from Soufrière Hills Volcano. However, a key result of the paper
39 was that the compositions of some plagioclase-hosted melt inclusions indicate mixing
40 of mafic magma components into the host andesite and trapping of the mixed melts
41 within phenocrysts. This interpretation is consistent with our earlier work on the
42 chemistry of melt inclusions (Humphreys et al. 2010) and of microlite crystal
43 populations (Humphreys et al. 2009; 2013). Humphreys et al. (2010) proposed this
44 interpretation by showing that a subset of Soufrière Hills melt inclusions and matrix
45 glasses has anomalous concentrations of K_2O and/or TiO_2 , as have mafic inclusion
46 matrix glasses (see figure 2, Humphreys et al. 2010). However, in their Appendix,
47 DR2014 suggest that enrichment in K_2O can only result from decompression
48 crystallisation and not from magma mingling. They also assert that our melt inclusion
49 dataset is fundamentally flawed and subject to faulty corrections for post-entrapment
50 correction; and that our melt inclusions were actually matrix glasses. Finally, DR2014
51 doubt “whether or not one can look at melt-inclusion analyses and distinguish the
52 effects of decompression crystallization... from the effects of mingling... with
53 components derived from the injected mafic magma”.

54

55 Here we address the criticisms of the DR2014 Appendix, drawing on additional
56 published data to support our arguments and explanations. We were unable to
57 reproduce some of the key figures in DR2014, so we present revised, corrected
58 versions. We demonstrate clearly the compositional effects of decompression
59 crystallization and discuss carefully how this can be distinguished from mingling.
60 Finally, we consider thoroughly, though ultimately reject, the suggestion that
61 enrichment of melt inclusions and matrix glasses in K_2O can only be derived from
62 slow crystallisation, and give our supporting arguments.

63

64 **Volatile contents of melt inclusions and matrix glasses**

65 Devine & Rutherford (2014) firstly called into question our estimates of melt volatile
66 contents for melt inclusions and matrix glasses, as published in Humphreys et al.
67 (2010), and suggested that some of our melt inclusions might actually be matrix

68 glasses. The volatile contents of the earliest erupted magmas at Soufrière Hills
69 Volcano (from 1996) were reported to be up to ~4.6 wt% H₂O based on ‘volatiles by
70 difference’ (VBD) from 100% analytical total by electron microprobe (Devine et al.
71 1998). This method has an uncertainty of approximately 0.6 wt% H₂O (Devine et al.
72 1995; Humphreys et al. 2006a). This result was supported by FTIR analyses of six
73 quartz-hosted melt inclusions (Barclay et al. 1998), with H₂O contents of 3.52 – 5.05
74 wt% and <60 ppm CO₂. We note that this paper (on which both Devine and
75 Rutherford were co-authors) also reports the volatile contents of two plagioclase-
76 hosted melt inclusions, as 4.7 wt% and 0 wt% H₂O. In comparison, our VBD
77 estimates of melt H₂O contents in pristine, plagioclase-hosted melt inclusions are
78 similar but range from 0 up to 8.2 wt% (Humphreys et al. 2010). Obtaining anhydrous
79 glass EPMA data with analytical totals in the region of 100% is consistent with the
80 propagated uncertainty of the electron probe analyses and the VBD method (Devine et
81 al. 1995; Humphreys et al. 2006a); for our dataset this fully propagated uncertainty
82 was typically 1.2 wt%. We ran a suite of hydrous glass secondary standards
83 (Humphreys et al. 2006a) at the same time as the unknowns and these give an average
84 absolute deviation of VBD relative to known H₂O of ~1 wt%. We agree that our
85 highest VBD values are probably an overestimate, but broadly, the high inferred H₂O
86 concentrations are supported by direct analysis of H₂O in a subset of the same
87 pumice-hosted inclusions by secondary ion mass spectrometry (SIMS), which gave
88 1.14 – 6.24 wt% H₂O (Humphreys et al. 2009a; figure 1). Likewise, FTIR
89 measurements by Mann et al. (2013) gave 1.2 to 6.7 wt% H₂O in quartz- and
90 plagioclase-hosted melt inclusions from pumices erupted in Vulcanian explosions
91 during 1997 and 2003-2004. These values are consistent with our earlier
92 measurements. We therefore do not consider our analyses to be a “divergence” from
93 the DR2014 dataset. There need be no expectation that the maximum volatile contents
94 of multiple aliquots of magma erupted over 15 years should be identical; melt
95 inclusion datasets from volcanoes globally commonly show variable H₂O contents
96 (e.g. Zimmer et al. 2010; Plank et al. 2013). However, the fact that the highest H₂O
97 contents were found in samples erupted in January 2007 by Humphreys et al. (2010),
98 and also in samples erupted in August 1997 by Mann et al. (2013) suggests that
99 maximum volatile contents have probably not changed substantially over the course
100 of the eruption. Suites of melt inclusions typically show a wide range of H₂O

101 contents, so the very limited data presented in the original work (Devine et al. 1998)
102 are entirely consistent with the more detailed, recent studies.

103

104 Our volatile data for pumice-hosted melt inclusions equate to entrapment pressures of
105 at least 220 MPa, or more if substantial CO₂ is present, for which there is good
106 evidence from both gas emissions and melt inclusion data (Edmonds et al. 2014).
107 Thus the melt inclusions define a range of pressures that is consistent with a vertically
108 protracted magma reservoir of the type inferred from seismic tomography and from
109 ground deformation (Elsworth et al 2008; Voight et al. 2010; Elsworth et al. 2014).
110 We interpreted the range of H₂O contents to be the result of differential entrapment
111 pressures of the melt inclusion suite during decompression crystallisation, as
112 previously proposed elsewhere including Shiveluch Volcano, Kamchatka (Humphreys
113 et al. 2006b; 2008), Mount St Helens (Blundy & Cashman 2005), Stromboli, Italy
114 (Metrich et al. 2001) and Jorullo, Mexico (Johnson et al. 2008) amongst others. This
115 is consistent with the low volatile contents found for matrix glass (generally less than
116 0.5 wt% H₂O; see below) and with the overall geochemical variations of the melt
117 inclusion and matrix glass data. These data show increasing concentrations of
118 incompatible elements (e.g. K, Ti, Mg) and decreasing concentrations of elements that
119 are compatible in plagioclase (e.g. Ca, Na) with increasing SiO₂. We accept that in
120 part this may be related to our application of corrections for post-entrapment
121 crystallisation, although this does not affect the key elements of interest (e.g. K, Ti,
122 Fe; see below for further discussion). However, the combined dataset for matrix
123 glasses (which of course are uncorrected) and melt inclusions is consistent with
124 progressive fractionation of plagioclase together with minor pyroxenes + oxides
125 during decompression (see figure 1 of Humphreys et al. 2010). This interpretation fits
126 with observations of substantial groundmass crystallisation of these same phases. The
127 compositions are also generally consistent with the results of phase equilibria
128 experiments of Couch et al. (2003) which resulted in crystallisation of plagioclase and
129 pyroxene (see later). We note that Mann et al. (2013) interpreted the variable H₂O
130 contents of melt inclusions to reflect hydrogen loss from the melt inclusions during
131 magma stalling in the conduit rather than variable entrapment pressures. However, the
132 co-variation of H₂O and Cl measured by SIMS (e.g. Humphreys et al. 2009a) in some
133 pumice-hosted melt inclusions would argue against this possibility, as Cl presumably

134 cannot be lost easily by diffusion through the host phenocryst but is known to degas
135 together with H₂O during decompression (e.g. Villemant & Boudon 1999).

136

137 We do not dispute that plagioclase-hosted melt inclusions in many Montserrat dome
138 samples (including those dome samples studied by Humphreys et al. 2010) may have
139 substantially or completely lost their water; they are ‘leaked’ melt inclusions and not
140 matrix glasses. This is the reason that we excluded these samples from our study of
141 H₂O and Cl degassing (Humphreys et al. 2009a). By comparison with the well
142 documented similar effect in both natural and experimental olivines (Hauri 2002;
143 Portnyagin et al. 2008; Gaetani et al. 2012) we infer that water loss may result from
144 diffusion of H through the host phenocryst, as demonstrated experimentally by
145 Johnson & Rossman (2013). The extent of diffusive loss likely depends on clast size
146 (Lloyd et al. 2013) as well as the permeability of the dome, and probably occurs
147 during prolonged storage at low pressures (perhaps in the lava dome itself) and at, or
148 close to, magmatic temperatures. We would anticipate that H loss through the host
149 phenocryst may explain anomalous trends in CO₂-H₂O space that are otherwise
150 attributed to re-equilibration with highly CO₂-rich vapours (e.g. Collins et al. 2009 for
151 olivine-hosted inclusions). If this is the case, we would also expect these inclusions to
152 have anomalously oxidising compositions (e.g. Gaetani et al. 2012; Humphreys et al.
153 in press).

154

155 **Corrections for post-entrapment crystallisation**

156 In the supplementary dataset to our previous study (Humphreys et al. 2010) we
157 provided petrographic information for each melt inclusion in our original dataset
158 (including a description of shape, colour, presence or absence of bubble, textural
159 association in the host phenocryst, area, equivalent radius and volume, area and
160 volume of any post-entrapment crystallisation if present, as well as the raw, PEC-
161 adjusted and normalised anhydrous compositions). We now also present
162 representative backscattered SEM images of typical inclusions in figure 2. We also
163 estimated the amount of post-entrapment crystallisation (PEC) in each melt inclusion,
164 and attempted to correct the melt inclusion compositions for the observed PEC. In our
165 explanation of the correction procedure we used the term ‘pristine’ to refer to melt
166 inclusions that were free from post-entrapment crystallisation and thus did not need
167 correction. For the other inclusions, our post-entrapment crystallisation procedure

168 followed that of Saito et al. (2005), as described in the supplementary information to
169 Humphreys et al. (2010). The method was indeed developed for basaltic melt
170 inclusions but the principle is not changed by the composition of the melt or host
171 phenocryst. For plagioclase-hosted melt inclusions in particular, it is not always clear
172 exactly what host composition is truly in equilibrium with the inclusion as the textures
173 may be complex; precisely defining the volume and surface area of the inclusions
174 may also be very difficult (Humphreys et al. 2008). For this reason, we used a
175 constant plagioclase composition of An₄₀ and made simplifying assumptions about the
176 melt inclusion shape. This may have introduced some uncertainty or error into the
177 corrected dataset, mainly for the key components of the host plagioclase (SiO₂, Al₂O₃,
178 CaO and Na₂O; see discussion above), although we also provided the uncorrected
179 compositions for reference. For completeness we show the effect of these corrections
180 in the haplogranite ternary Ab-Or-Q (figure 3). However, we argue that for the minor
181 elements of particular interest to this discussion, i.e. FeO, TiO₂ and K₂O, the PEC
182 correction makes no significant difference.

183

184 DR2014 commented on the presence of normative Wo in some corrected melt
185 inclusion compositions. All our compositions plotted were suitable for plotting in the
186 haplogranite projection following Blundy & Cashman (2001), which requires glasses
187 with < 20 wt% normative anorthite. All our published glasses have ≤16 wt%
188 normative anorthite but typical values are <<10 wt%. Normative wollastonite is
189 calculated for a minority of compositions but this amounts to an average of 0.85 wt%
190 ± 0.54 normative Wo. This amount of normative Wo is equivalent to a very minor
191 shift in the position of a few glasses within the haplogranite ternary, away from the
192 Qz'' apex (a shift smaller than the size of the symbols in figure 2). If anything, this
193 may show that our PEC-corrected compositions have slightly overestimated CaO
194 concentrations, but this does not affect the nature of our interpretations, which are
195 largely based on minor element compositional variations. We would also add that
196 many of DR2014's own data show just as high dispersion in the haplogranite
197 projection as ours (e.g. DR2014 figure 19A.6 and 19A.7) and that our data are not
198 unique in having a small amount of normative wollastonite (see also Edmonds et al.
199 2002; Mann et al. 2013).

200

201 **The anomalous groundmass composition of Soufrière Hills magma**

202 Figure 19A.11 of DR2014 shows the anomalous composition of the bulk groundmass
203 from Soufrière Hills magma, as recognised by several authors previously. Although
204 DR2014 state that this may be due to analytical artefacts caused by inaccurate raster
205 analysis of inhomogeneous groundmass, there are alternative explanations. One is that
206 the groundmass is contaminated by disaggregation of mafic enclaves and transfer of
207 small crystals into the andesite groundmass, including clinopyroxene and Ca-rich
208 plagioclase (Humphreys et al. 2009b; 2013). This is consistent with the interpretation
209 that the anomalous glass compositions may be related to hybridisation; see below
210 (Humphreys et al. 2010; Devine & Rutherford 2014). It has also been suggested that
211 the bulk groundmass composition could be affected by incorporation of substantial
212 additional SiO₂ through precipitation of cristobalite in vesicles (Horwell et al. 2012).

213

214 **K₂O enrichment during slow decompression crystallisation?**

215 The substantive criticism of DR2014 about our earlier work is that the variably high
216 K₂O contents seen in a subset of our matrix glasses and melt inclusions may be
217 related to slow crystallisation of the andesite during ascent and decompression, rather
218 than to hybridisation with mafic enclave components as we suggested (Humphreys et
219 al. 2010). Occasional high-K glasses can also be observed in several previous studies
220 of SHV eruptive products and include matrix glasses and melt inclusions in both
221 plagioclase and hornblende (e.g. Edmonds et al. 2002; Harford et al. 2003; and in
222 particular Buckley et al. 2006). Anomalous high-K melt inclusions have also been
223 observed at Colima Volcano, Mexico, where they have been ascribed to recording
224 heterogeneity in the melt caused by the breakdown of amph-bt cumulate nodules
225 (Reubi & Blundy 2008). In our earlier work we considered this process, alongside the
226 breakdown of amphibole during heating or decompression (Buckley et al. 2006), but
227 concluded that this could not fully explain either the compositions or the textural
228 associations of the glasses. We also considered the possibility of entrapment of
229 anomalous boundary layer melts into melt inclusions (Baker 1991) but rejected this on
230 the basis that matrix glasses were also affected.

231

232 The suggestion of DR2014 that K₂O variability in matrix glasses and melt inclusions
233 could be due to variations in magma ascent rate (and thus extent of decompression
234 crystallisation) is interesting. This was based on experiments conducted by Hammer
235 & Rutherford (2002), which produced high-K, low-Na glasses through decompression

236 crystallization of plagioclase. In their experiments, isothermal decompression of
237 Pinatubo dacite resulted in groundmass crystallisation of plagioclase + quartz, with
238 other phases in minor abundance. K_2O is essentially incompatible in these phases, so
239 K_2O contents of the experimental matrix glasses increase with increasing groundmass
240 crystallinity, accompanied by decreasing CaO, which is compatible in plagioclase. In
241 those experiments, increasing the dwell time at the final pressure actually resulted in a
242 greater *spread* of K_2O contents, rather than a uniform increase. However, the same
243 trend of increasing K_2O and decreasing CaO is also observed, more clearly, in the
244 experimental studies of Martel & Schmidt (2003), Couch et al. (2003) and Brugger &
245 Hammer (2010). The experiments of Martel & Schmidt (2003) are particularly
246 appropriate because their starting material was chosen to have the composition of the
247 most evolved (i.e. highest SiO_2 on an anhydrous basis) plagioclase-hosted melt
248 inclusions from Devine et al. (1998), equivalent to melts in equilibrium with
249 phenocryst rims during decompression crystallisation (Martel & Schmidt 2003). In all
250 sets of experiments, the very high-K compositions are achieved only at very low final
251 pressures (e.g. 15 MPa, Martel & Schmidt 2003; <25 MPa, Hammer & Rutherford
252 2002; <20 MPa, Brugger & Hammer 2010), presumably as the melt approaches
253 saturation in K-feldspar. The strong decrease in CaO that accompanies K_2O
254 enrichment has important implications for plagioclase-melt thermometry (Humphreys
255 et al. 2014).

256

257 DR2014 rightly point out that we do not find both high-K and low-K *matrix glasses* in
258 the same sample. However, we do find both high-K and low-K melt inclusions in the
259 same sample, *and* in the same crystal. Although our most evolved matrix glass
260 compositions are similar to the very low pressure, high-K experimental glasses
261 (figures 4, 5), it seems clear that slow, low-pressure decompression crystallisation
262 cannot explain the enrichment of those compositions in TiO_2 (figure 4). Specifically,
263 the experiments show that the very high K_2O contents can only be reached after
264 extensive crystallisation at low pressure, resulting in extremely low CaO and MgO or
265 FeO concentrations; this is not consistent with the spread to higher CaO and FeO at
266 high K_2O contents. We therefore conclude that the most likely explanation for the
267 anomalous, high-K melt compositions is still that of hybridisation with mafic-derived
268 melt components.

269

270 **Compositions of mafic enclave glasses**

271 The compositional overlap of high-K melt inclusions and matrix glasses with mafic
272 enclave glasses led us to propose that the anomalous, high-K glasses were derived
273 from disaggregation of mafic material and hybridisation with the andesite
274 (Humphreys et al. 2010). This would be consistent with similar observations made on
275 the compositions of microlite crystal populations (Humphreys et al. 2009b; 2013). In
276 our original study, the key observation was that both K_2O and TiO_2 anomalies are
277 observed in melt inclusions and matrix glasses, and that they were apparently
278 decoupled (see figure 2 of Humphreys et al. 2010). This decoupling led us to propose
279 our model of diffusive fractionation, based on the facts that a) K and Ti are enriched
280 in mafic enclave glasses relative to residual liquids in the andesite, generating a
281 chemical gradient, and b) the diffusivity of K in melt is significantly faster than that of
282 Ti (e.g. Bindeman & Davis 1999, Richter et al. 2003) raising the possibility for
283 fractionation. In the main body of their paper, DR2014 supported our interpretation
284 that the variance of glass chemistry was caused by disaggregation and mixing with
285 mafic-derived components, though they based this on FeO contents in addition to
286 TiO_2 . Their issue with our interpretation seems to arise from the fact that their mafic
287 enclave glasses were not enriched in K_2O , whereas ours were (figures 4-6). We have
288 discussed the possible alternative for K-enrichment, that of low pressure
289 crystallisation, above. If this were the controlling influence on mafic glass
290 composition, comparison with experimental studies would imply that the mafic
291 enclaves studied by DR2014 were quenched at very high pressure (~200 MPa)
292 whereas those studied by Humphreys et al. (2010) quenched over a range of
293 pressures, but below ~35 MPa; this seems implausible.

294

295 An alternative explanation is offered by compositions reported by more recent work
296 (Mann 2010; Plail et al. 2014; Plail, 2014). Plail et al. (2014) identified two texturally
297 and geochemically distinct types of mafic enclaves in Phase 5 of the eruption (rocks
298 erupted during 2009-2010), as well as a third type that was a hybrid of the first two.
299 Type A enclaves are glassy and vesicular, with more mafic compositions, and the
300 framework-forming phase is high-Al amphibole. Type B enclaves are more evolved
301 (less mafic, with higher SiO_2) in composition, with higher crystallinity and lower
302 vesicularity; the framework-forming phase is plagioclase and high-Al amphibole is
303 rare to absent (Plail et al. 2014). Type A enclaves are thought to form by rapid

304 thermal equilibration and vesiculation of the enclave magma during injection into the
305 andesite. Type B enclaves were inferred to have resulted from significant
306 hybridisation of enclave magma with the andesite, associated with slower cooling
307 (Plail et al. 2014). The two types of mafic enclaves have very different residual matrix
308 glass compositions, even for enclaves erupted in the same andesite magma (Plail et al.
309 2014). Type A enclaves are characterised by variably high FeO, TiO₂ and MgO. Type
310 B enclaves have compositions that are more similar to the host andesite matrix glass
311 (figure 4). Importantly, the rapidly quenched, primitive Type A enclaves show strong
312 enrichment in K₂O, whereas the more slowly crystallised Type B are only slightly
313 enriched (figure 4). Figures 4-6 show clearly the disparity between Type A and Type
314 B mafic enclave glasses.

315

316 Devine & Rutherford (2014) suggested that the difference between their mafic
317 enclave analyses and ours (see DR2014 figure 19A.10) is because the mafic enclaves
318 in our study had undergone slower crystallisation in the conduit, resulting in a spread
319 towards K₂O enrichment. In fact, the comparison with additional data shows that the
320 DR2014 mafic glass compositions are unusual in having particularly high TiO₂ and
321 FeO concentrations, yet no K₂O enrichment (figures 5,6). The contrast in Type A and
322 Type B enclave glasses also suggests that variations in decompression rate are
323 unlikely to be the cause for the observed compositional differences, as the most K₂O-
324 enriched (Type A) enclave glasses are derived from enclaves that quenched rapidly
325 (Plail et al. 2014), not those that crystallised slowly. Based on minor element
326 compositional variations (figures 4 and 5), we therefore suggest that it is more likely
327 that the Soufrière Hills magma system is regularly fluxed by mafic melts of variable
328 composition. This should be investigated further using trace elements and isotopic
329 compositions, to investigate possible heterogeneity in the magma source regions and
330 thus melt generation processes.

331

332 **Conclusions**

333 We have thoroughly reviewed the melt inclusion dataset presented by Humphreys et
334 al. (2010) and showed the results to be robust. High volatile contents inferred ‘by
335 difference’ from electron microprobe analysis are supported by direct measurements
336 in multiple independent studies. Plagioclase-hosted melt inclusions in many dome
337 lavas have low H₂O contents, which we attribute to diffusive loss through the host

338 mineral. The anomalous K₂O-enrichment found in a subset of our melt inclusions and
339 matrix glasses is supported by several other independent studies, and can be best
340 explained as a result of mingling and hybridisation with mafic magma, as originally
341 proposed. Our corrections for post-entrapment crystallisation did not introduce
342 significant artefacts into the dataset that would contradict these conclusions.
343 Additional mafic glass data from the recent literature shows that instead, intruding
344 mafic magmas at Soufrière Hills were probably variable in composition; we therefore
345 recommend further investigation using trace elements and isotopes.

346

347

348 **Acknowledgements**

349 This work benefited from helpful journal reviews by Philipp Ruprecht, Mary-Jo
350 Brounce and Kathy Cashman. MCSH was supported by a Royal Society University
351 Research Fellowship.

352

353

354 **References**

355 Barclay, J., Rutherford, M.J., Carroll, M.R., Murphy, M.D., Devine, J.D., Gardner, J.
356 & Sparks, R.S.J. (1998) Experimental phase equilibria constraints on pre-eruptive
357 storage conditions of the Soufrière Hills magma. *Geophysical Research Letters* **25**,
358 3437-3440

359 Bindeman, I.N. & Davis, A.M. (1999) Convection and redistribution of alkalis and
360 trace elements during the mingling of basaltic and rhyolitic melts. *Petrology* **7**, 91-101

361 Blundy, J. & Cashman, K. (2005) Rapid decompression-driven crystallization
362 recorded by melt inclusions from Mount St. Helens volcano. *Geology* **33**, 793-796

363 Blundy, J. & Cashman, K. (2001) Ascent-driven crystallisation of dacite magmas at
364 Mount St Helens, 1980-1986. *Contributions to Mineralogy & Petrology* **140**, 631-650

365 Buckley, V.J.E., Sparks, R.S.J. & Wood, B.J. (2006) Hornblende dehydration
366 reactions during magma ascent at Soufrière Hills Volcano, Montserrat. *Contributions*
367 *to Mineralogy & Petrology* **151**, 121-140

368 Cashman, K.V. (1992) Groundmass crystallization of Mount St. Helens dacite, 1980-
369 1986: a tool for interpreting shallow magmatic processes. *Contributions to*
370 *Mineralogy & Petrology* **109**, 431-449

371 Devine, J.D., Gardner J.E., Brack, H.P., Layne, G.D. & Rutherford, M.J. (1995)
372 Comparison of microanalytical methods for estimating H₂O contents of silicic
373 volcanic glasses. *American Mineralogist* **80**, 319-328

374 Devine, J.D., Murphy, M.D., Rutherford, M.J., Barclay, J., Sparks, R.S.J., Carroll,
375 M.R., Young, S.R. & Gardner, J.E. (1998). Petrologic evidence for pre-eruptive
376 pressure-temperature conditions, and recent reheating, of andesitic magma erupting at
377 the Soufrière Hills Volcano, Montserrat, W.I. *Geophysical Research Letters* **25**, 3669-
378 3672

379 Devine, J.D. & Rutherford, M.J. (2014) Magma storage region processes of the
380 Soufrière Hills Volcano, Montserrat. *Geological Society, London, Memoirs* **39**, 361-
381 381

382 Edmonds, M., Pyle, D. & Oppenheimer, C. (2001) A model for degassing at the
383 Soufrière Hills Volcano, Montserrat, West Indies, based on geochemical data. *Earth*
384 *and Planetary Science Letters* **186**, 159-173

385 Edmonds, M., Pyle, D. & Oppenheimer, C. (2002) HCl emissions at Soufrière Hills
386 Volcano, Montserrat, West Indies, during a second phase of dome building:
387 November 1999 to October 2000. *Bulletin of Volcanology* **64**, 21-30

388 Edmonds, M., Humphreys, M.C.S., Hauri, E.J., Herd, R.A., Wadge, G., Rawson, H.,
389 Ledden, R., Plail, M., Barclay, J., Aiuppa, A., Christopher, T.E., Giudice, G. & Guida,
390 R. (2014) Pre-eruptive vapour and its role in controlling eruption style and longevity
391 at Soufrière Hills Volcano. *Geological Society, London, Memoirs* **39**, 291-315

392 Elsworth, D., Mattioli, G., Taron, J., Voight, B. & Herd, R. (2008) Implications of
393 magma transfer between multiple reservoirs on eruption cycling. *Science* **322**, 246-
394 248

395 Elsworth, D., Foroozan, R., Taron, J., Mattioli, G.S. & Voight, B. (2014) Geodetic
396 imaging of magma migration at Soufrière Hills Volcano 1995 to 2008. *Geological*
397 *Society, London, Memoirs* **39**, 219-227

398 Gaetani, G., O'Leary, J.A., Shimizu, N., Bucholz, C.E. & Newville, M. (2012) Rapid
399 reequilibration of H₂O and oxygen fugacity in olivine-hosted melt inclusions.
400 *Geology* doi: 10.1130/G32992.1

401 Hammer, J.E. & Rutherford, M.J. (2002) An experimental study of the kinetics of
402 decompression-induced crystallization in silicic melt. *Journal of Geophysical*
403 *Research* **107**, doi: 10.1130/G32992.1

404 Harford, C.L., Sparks, R.S.J. & Fallick, A.E. (2003) Degassing at the Soufrière Hills
405 Volcano, Montserrat, recorded in matrix glass compositions. *Journal of Petrology* **44**,
406 1503-1523

407 Hauri, E. (2002) SIMS analysis of volatiles in silicate glasses, 2: isotopes and
408 abundances in Hawaiian melt inclusions. *Chemical Geology* **183**, 115-141

409 Horwell, C.J., Williamson, B.J., Llewellyn, E.W., Damby, D.E. & Le Blond, J.S.
410 (2013) The nature and formation of cristobalite at the Soufrière Hills volcano,
411 Montserrat: implications for the petrology and stability of silicic lava domes. *Bulletin*
412 *of Volcanology* **75**, 696-

413 Humphreys, M.C.S., Kearns, S.L. & Blundy, J.D. (2006a) SIMS investigation of
414 electron-beam damage to hydrous, rhyolitic glasses: Implications for melt inclusion
415 analysis. *American Mineralogist* **91**, 667-679

416 Humphreys, M.C.S., Blundy, J.D. & Sparks, R.S.J. (2006b) Magma evolution and
417 open-system processes at Shiveluch Volcano: Insights from phenocryst zoning.
418 *Journal of Petrology* **47**, 2303-2334

419 Humphreys, M.C.S., Blundy, J.D. & Sparks, R.S.J. (2008) Shallow-level
420 decompression crystallisation and deep magma supply at Shiveluch Volcano.
421 *Contributions to Mineralogy and Petrology* **155**, 45-61

422 Humphreys, M.C.S., Edmonds, M., Christopher, T. & Hards, V. (2009a) Chlorine
423 variations in the magma of Soufrière Hills volcano, Montserrat: Insights from Cl in
424 hornblende and melt inclusions. *Geochimica et Cosmochimica Acta* **73**, 5693-5708

425 Humphreys, M.C.S., Christopher, T. & Hards, V. (2009b) Microlite transfer by
426 disaggregation of mafic inclusions following magma mixing at Soufrière Hills
427 volcano, Montserrat. *Contributions to Mineralogy & Petrology* **157**, 609-624

428 Humphreys, M.C.S., Edmonds, M., Christopher, T. & Hards, V. (2010) Magma
429 hybridisation and diffusive exchange recorded in heterogeneous glasses from
430 Soufrière Hills Volcano, Montserrat. *Geophysical Research Letters* **37**, L00E06

431 Humphreys, M.C.S., Edmonds, M., Plail, M., Barclay, J., Parkes, D. & Christopher,
432 T. (2013) A new method to quantify the real supply of mafic components to a hybrid
433 andesite. *Contributions to Mineralogy and Petrology* **165**, 191-215

434 Humphreys, M.C.S., Kloecking, M. & Edmonds, M. (2014). The fidelity of
435 plagioclase-melt thermometry for decompression-driven magma crystallisation.
436 Goldschmidt conference 2014, abstract no. 1639.

437 Johnson, E.R., Wallace, P.J., Cashman, K.V., Delgado Granados, J. & Kent, A.J.R.
438 (2008). Magmatic volatile contents and degassing-induced crystallization at Volcan
439 Jorullo, Mexico: Implications for melt evolution and the plumbing systems of
440 monogenetic volcanoes. *Earth and Planetary Science Letters* **269**, 478-487

441 Johnson, E.A. & Rossman, G.R. (2013) The diffusion behaviour of hydrogen in
442 plagioclase feldspar at 800-1000 °C: Implications for re-equilibration of hydroxyl in
443 volcanic phenocrysts. *American Mineralogist* **98**, 1779-1787

444 Mann, C.P. (2010) Magma chamber dynamics at Soufrière Hills volcano, Montserrat.
445 Unpublished PhD thesis, McGill University.

446 Mann, C.P., Wallace, P.J. & Stix, J. (2013) Phenocryst-hosted melt inclusions record
447 stalling of magma during ascent in the conduit and upper magma reservoir prior to
448 vulcanian explosions, Soufrière Hills volcano, Montserrat, West Indies. *Bulletin of*
449 *Volcanology* **75**, 687

450 Metrich, N., Bertagnini, A., Landi, P. & Rosi, M. (2001) Crystallization driven by
451 decompression and water loss at Stromboli Volcano (Aeolian Islands, Italy). *Journal*
452 *of Petrology* **42**, 1471-1490

453 Plail, M. (2014) Geochemical and petrological investigation into the magmatic system
454 at Soufrière Hills Volcano, Montserrat. Unpublished PhD thesis, University of East
455 Anglia, UK.

456 Plail, M., Barclay, K., Humphreys, M.C.S., Edmonds, M., Herd, R.A. & Christopher,
457 T.E. (2014) Characterization of mafic enclaves in the erupted products of Soufrière

458 Hills Volcano, Montserrat, 2009 to 2010. Geological Society, London, Memoirs **39**,
459 343-360

460 Portnyagin, M., Almeev, R., Matveev, S. & Holtz, F. (2008) Experimental evidence
461 for rapid water exchange between melt inclusions in olivine and host magma. Earth
462 and Planetary Science Letters **272**, 541-552

463 Reubi, O. & Blundy, J. (2008) Assimilation of plutonic roots, formation of high-K
464 'exotic' melt inclusions and genesis of andesitic magmas at Volcan de Colima,
465 Mexico. Journal of Petrology **49**, 2221-2243

466 Richter, F.M., Davis, A.M., De Paolo, D.J. & Watson, E.B. (2003) Isotope
467 fractionation by chemical diffusion between molten basalt and rhyolite. Geochimica
468 et Cosmochimica Acta **67**, 3905-3923

469 Saito, G., Uto, K., Kazahaya, K., Shinohara, H., Kawanabe, Y., Satoh, H. (2005).
470 Petrological characteristics and volatile content of magma from the 2000 eruption of
471 Miyakejima Volcano, Japan. Bulletin of Volcanology **67**, 268-280

472 Villemant, B. & Boudon, G. (1999). H₂O and halogen (F, Cl, Br) behaviour during
473 shallow magma degassing processes. Earth and Planetary Science Letters **168**, 271-
474 286

475 Voight, B., Widiwijayanti, C., Mattioli, G., Elsworth, D., Hidayat, D. & Strutt, M.
476 (2010) Magma-sponge hypothesis and stratovolcanoes: Case for a compressible
477 reservoir and quasi-steady deep influx at Soufrière Hills Volcano, Montserrat.
478 Geophysical Research Letters **37**, L00E05

479

480

481 **Figure captions**

482 Figure 1. Comparison of volatile contents estimated by secondary ion mass
483 spectrometry (SIMS) and ‘by difference’ from electron microprobe totals, for melt
484 inclusions from Humphreys et al. (2009a).

485

486 Figure 2. Back-scattered electron SEM images for typical melt inclusions. White
487 arrows mark inclusions analysed.

488

489 Figure 3. Haplogranite ternary projection showing melt inclusion and matrix glass
490 datasets discussed in the text. Black arrow illustrates effect of 10% post-entrapment
491 crystallisation correction. Red squares: Humphreys et al. (2010) melt inclusions, PEC-
492 corrected. Black open circles: Humphreys et al. (2010) matrix glasses. Orange circles:
493 Devine & Rutherford (2014) melt inclusions and matrix glasses. Black solid bars:
494 Mann et al. (2013) melt inclusions. Blue crosses: Couch et al. (2003) experimental
495 glasses.

496

497 Figure 4. Variation of K_2O and TiO_2 concentrations in melt inclusions and matrix
498 glasses from Soufrière Hills Volcano, equivalent to figure 2 of Humphreys et al.
499 (2010). Red squares: Humphreys et al. (2010) melt inclusions. Open circles:
500 Humphreys et al. (2010) matrix glasses. Blue diamonds: Humphreys et al. (2010)
501 mafic enclave glasses. Red circles: Devine & Rutherford (2014) mafic enclave
502 glasses. Solid black bars: Mann et al. (2013) melt inclusions. Open black squares:
503 Mann et al. (2013) mafic enclave glasses. Black crosses: Plail et al. (2014) Type A
504 mafic enclave glasses. Black asterisks: Plail et al. (2014) Type B mafic enclave glass.
505 Black filled squares: matrix glasses from Harford et al. (2003). Grey fields show the
506 compositional space of experimental glasses from Martel & Schmidt (2003) and
507 Couch et al. (2003), and the matrix glass and melt inclusion data of Buckley et al.
508 (2006).

509

510 Figure 5. Variation of (a) CaO vs K_2O and (b) FeO vs K_2O concentration in melt
511 inclusions and matrix glasses from Soufrière Hills Volcano. Symbols as in figure 4.
512 Grey fields are as in figure 4; black arrow and numbers denote the effect of
513 decreasing pressure in the Martel & Schmidt experiments, with approximate

514 equilibration pressures in MPa. Extremely low pressure crystallisation is required to
515 produce residual matrix glasses with strongly enriched K₂O contents.

516

517 Figure 6. Haplogranite ternary showing variation in mafic enclave glass compositions.

518 Symbols as in figure 4.

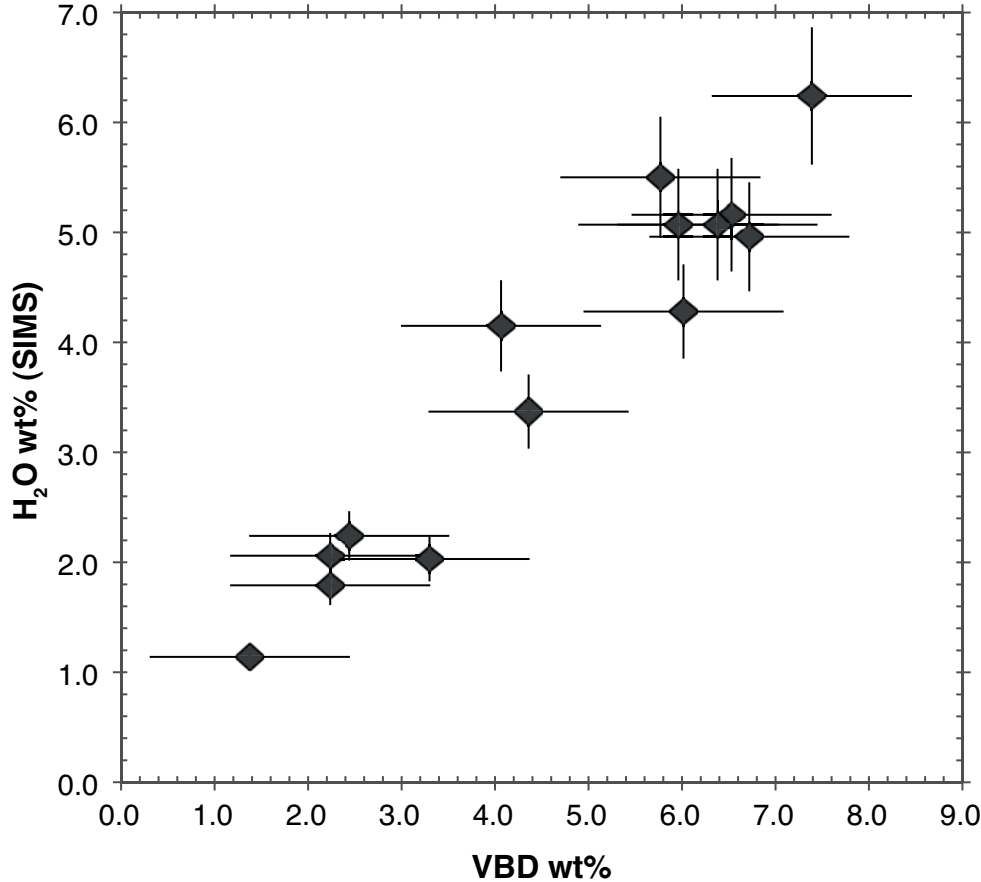


Figure 1

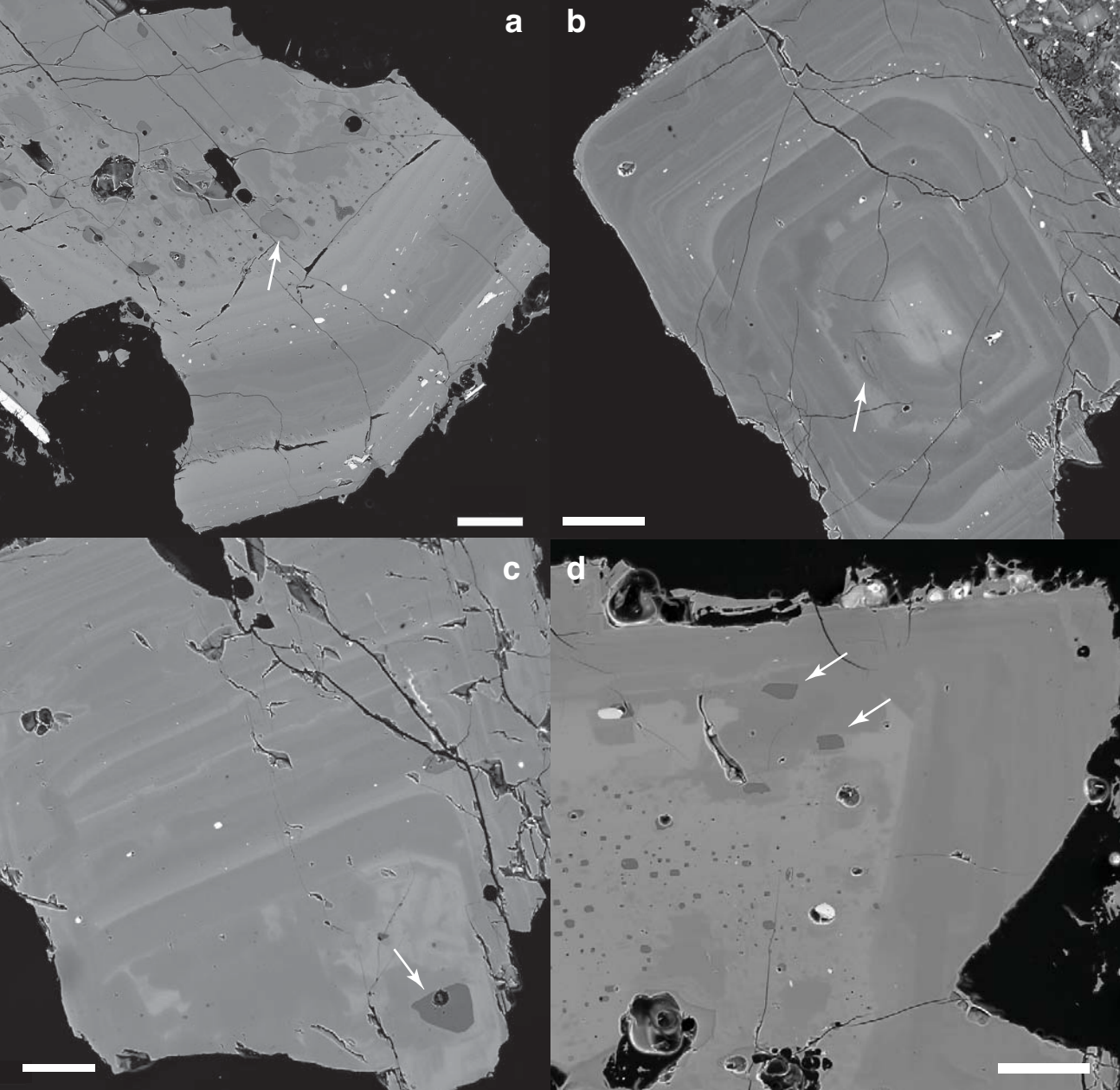


Figure 2

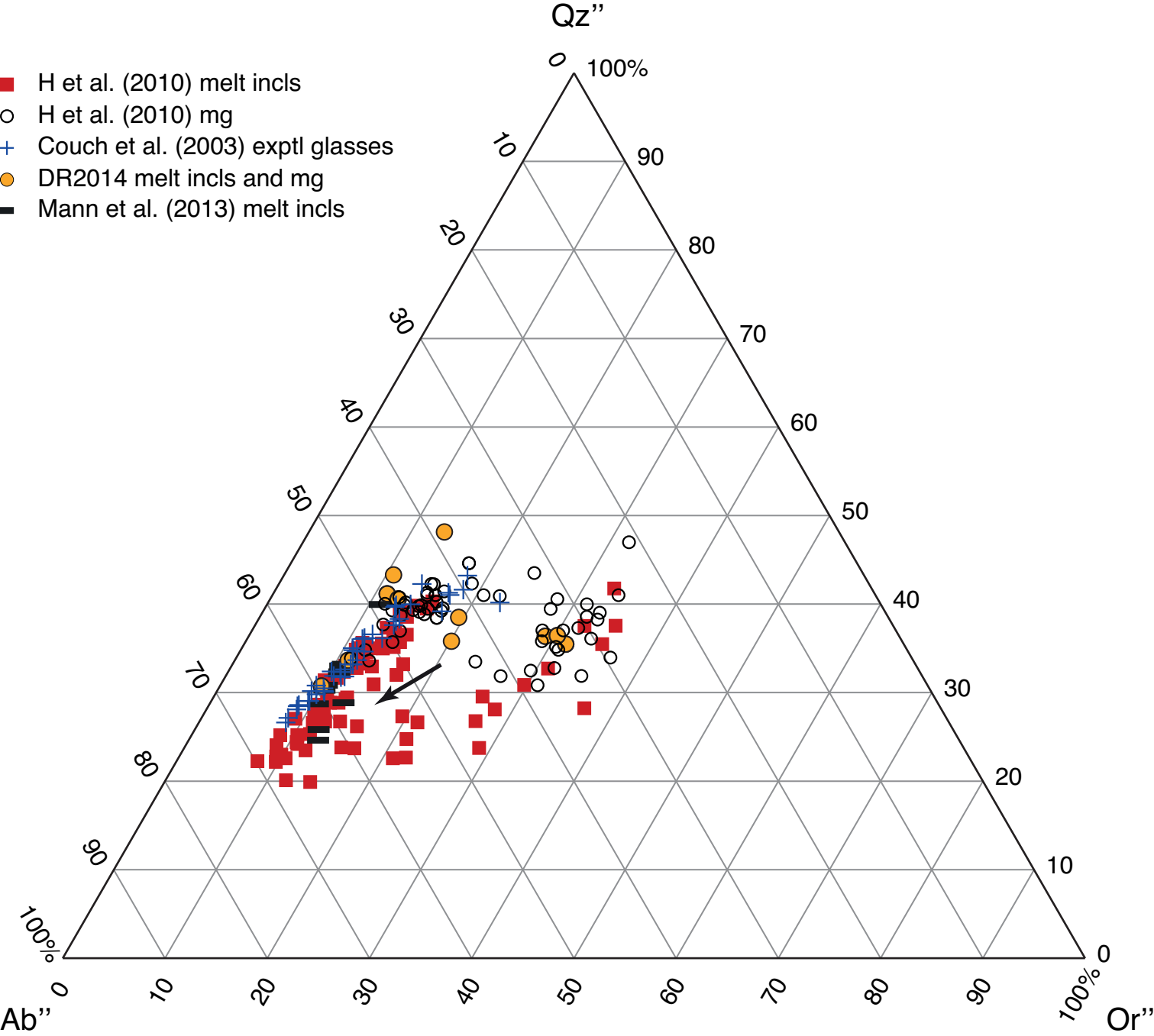


Figure 3

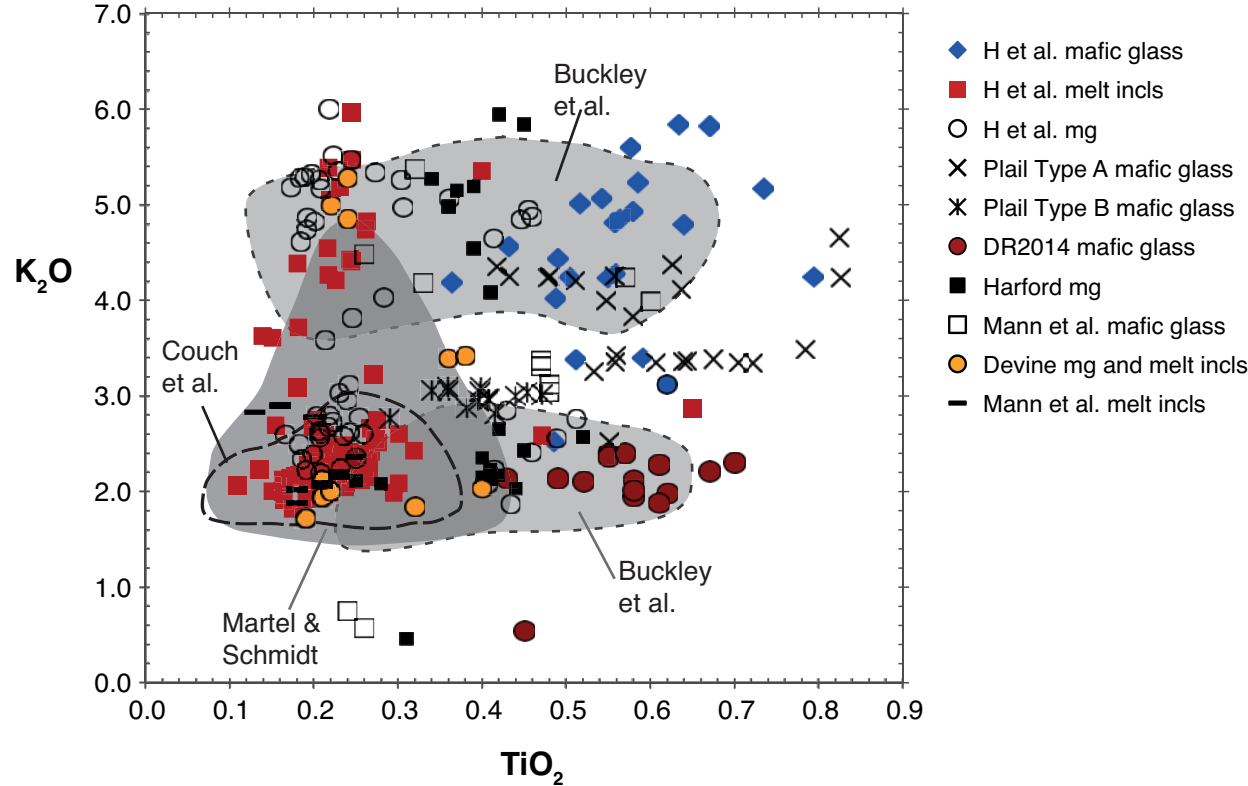


Figure 4

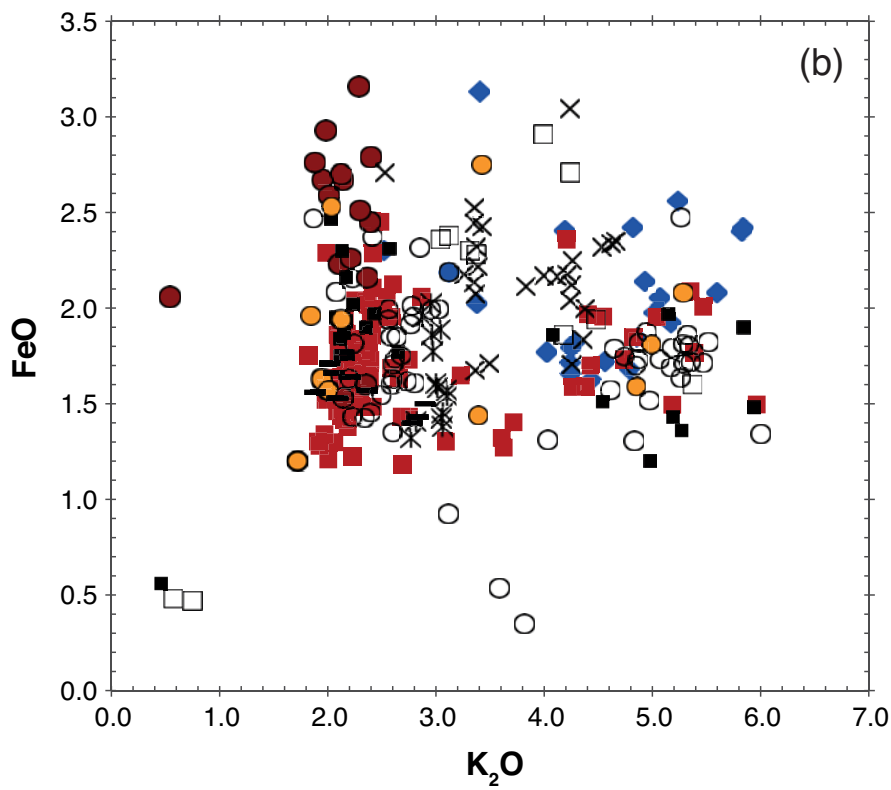
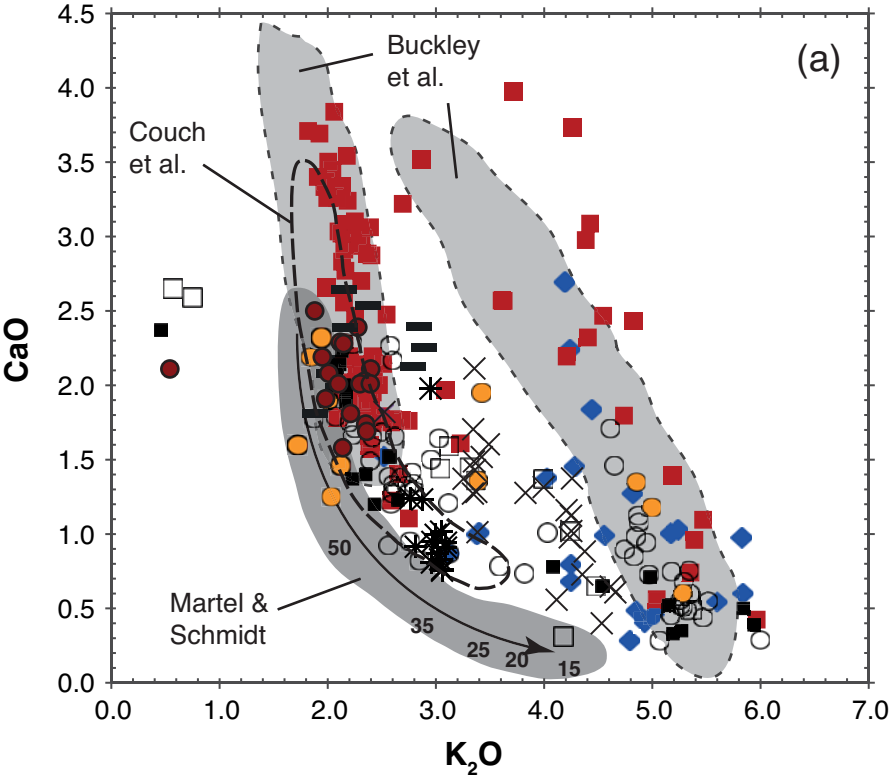


Figure 5

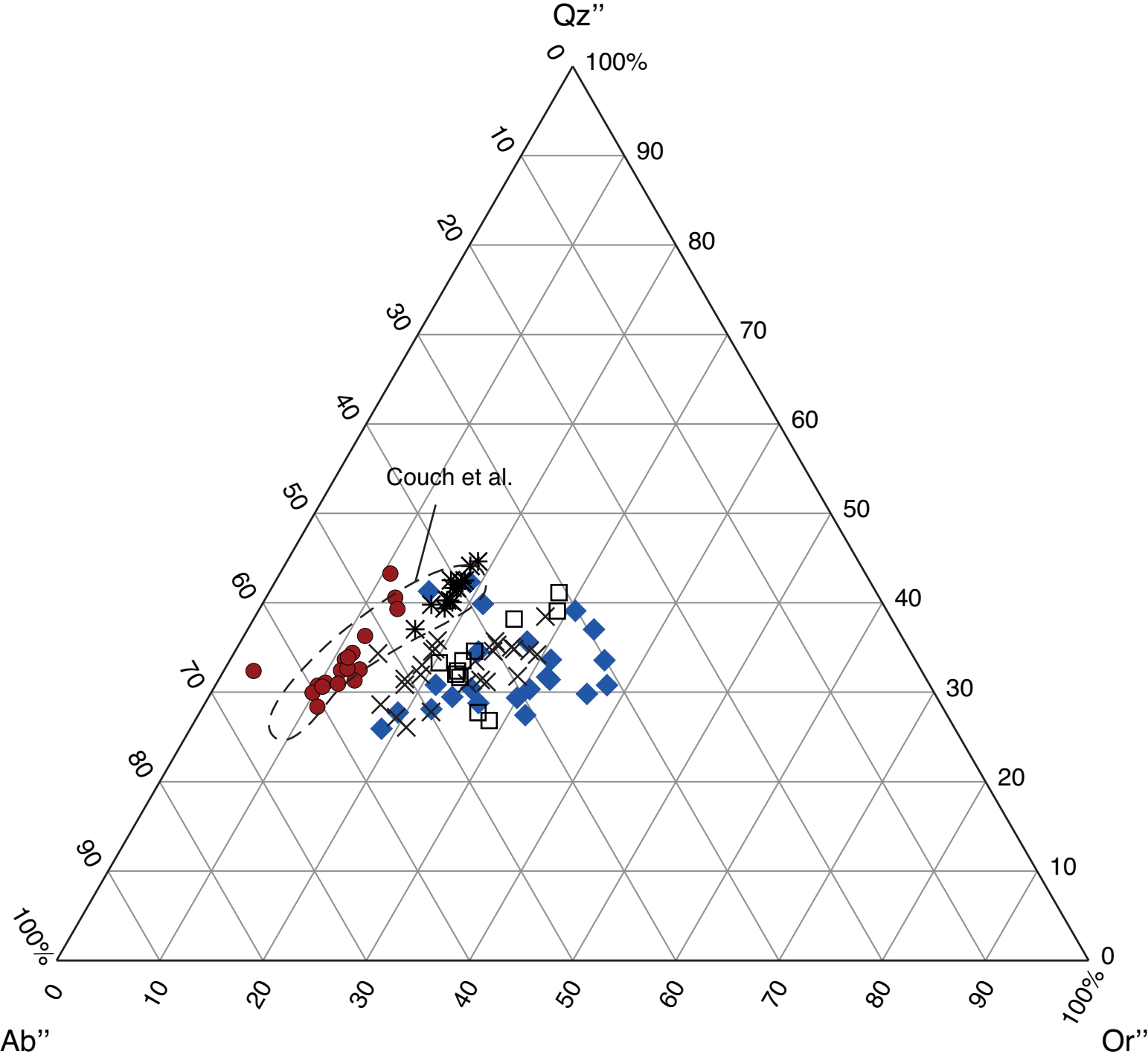


Figure 6